Shell-Restricted Swelling and Core Compression in Poly(*N*-isopropylacrylamide) Core−Shell Microgels

Clinton D. Jones and L. Andrew Lyon*

School of Chemistry and Biochemistry, Georgia Institute of Technology, Atlanta, Georgia 30332-0400

Received July 10, 2002

ABSTRACT: We report on an investigation of the structural relationship between the core and shell components in stimuli-sensitive core/shell microgels. Photon correlation spectroscopy measurements indicate that the presence of the shell alters the extent of core swelling. Core particles composed of poly(*N*-isopropylacrylamide-*co*-acrylic acid) (pNIPAm-*co*-AAc) undergo volume changes as a function of temperature and pH, where deprotonation of the acidic sites results in a volume increase (particle swelling). The addition of a poly(*N*-isopropylacrylamide) (pNIPAm) shell restricts the core from swelling to its native volume both above and below the pK_a of acrylic acid. Furthermore, the pH responsive core undergoes only small temperature-induced volume changes above the characteristic lower critical solution temperature (LCST) of pNIPAm (31 °C) at pH values where the acid groups are fully deprotonated. The addition of a pNIPAm shell results in compression of the core and induces a large volume change at the pNIPAm LCST. These effects are dependent on the degree of cross-linking in the core and shell. Particles synthesized with lower concentrations of *N*,*N*′-methylenebis(acrylamide) display greater degrees of shell-restricted swelling and compression upon the addition of a pNIPAm shell with an identical cross-linker concentration. These results are interpreted in terms of a previously proposed radial cross-linker density gradient, which places topological restraints upon the core following shell addition.

Introduction

Responsive hydrogel nanoparticles (microgels) are cross-linked, spherical, colloidal particles ranging in diameter from 10 to 1000 nm. Each particle is comprised of a random network of polymer chains that have the ability to exist in a swollen or collapsed state, depending on local solution conditions.[1,2] Perhaps the most widely studied responsive microgels are composed of the environmentally responsive polymer poly(*N*-isopropylacrylamide) (pNIPAm), which undergoes a temperature-induced, reversible phase transition at 31 °C.[2] Because of the chemical versatility and physical properties of pNIPAm-based microgels, particle design has continued to attract attention for potential applications in such fields as sensing,[3] drug delivery,[4] catalysis,[5] and pollution control.[6] Our approach to particle design involves the creation of core/shell microgels composed of environmentally responsive polymers in both the core and shell components. Polymer particles possessing a core/shell type morphology have recently been demonstrated to be viable as potential drug carriers,[7,8] to have biomimetic functions,[9] and to be applicable in advanced assembly processes.[10]

Our group has recently shown the viability of core/shell microgels in fundamental studies of particles displaying multiple volume phase transitions[11] along with investigating the dynamics and pathways of particle phase transitions.[12,13] The core/shell structure is evident from photon correlation spectroscopy (PCS) by monitoring size differences between the core and core/shell particles.[11,13] In the absence of complicating factors such as the pH-dependent data presented below, core/shell particles possess a larger hydrodynamic radius than the parent core, with the size increase being dependent on the mass of the shell hydrogel added to the core. We have also shown evidence of the core/shell structure via electron microscopy.[11] In that case, a negative staining technique was used to differentiate the core and shell components. Fluorescence investigations have indicated that the interface between the core and shell components lacks a large degree of interpenetration, as resonant energy transfer between core-localized donor fluorophores and shell-localized acceptors was observed to be quite small in the fully swollen state of the microgel.[12]

While the above examples illustrate some of the utility of the core/shell approach, a detailed understanding of the structure−function relationships for core/shell microgels is essential for the design of systems for true applications. In the present work, we show evidence that the swelling of the core component is modulated following addition of the shell. This is verified with photon correlation spectroscopy (PCS) by observing the volume phase transition behavior as a function of temperature and pH for pNIPAm-*co*-AAc (core)/pNIPAm (shell) microgels possessing various cross-linker densities. This particular core/shell design allows examination of particle volume changes isothermally as a function of pH in order to elucidate the impact that the added shell has on the swelling properties of the core. The impact of the shell component is concurrently monitored as a function of temperature and pH, showing that the shell greatly determines the phase transition behavior of the core even under solution conditions in which the core is charged above the AAc pK_a.

Experimental Section

Materials. All reagents were purchased from Sigma-Aldrich unless otherwise noted. *N*-Isopropylacrylamide (NIPAm) was recrystallized from hexanes (J.T. Baker) and dried in vacuo prior to use. Acrylic acid (AAc) was distilled under reduced pressure. *N*,*N*′-Methylenebis(acrylamide) (BIS), sodium dodecyl sulfate (SDS), and ammonium persulfate (APS) were all used as received. Water for all reactions, solution preparation,

* To whom correspondence should be addressed: e-mail lyon@chemistry.gatech.edu.

10.1021/ma021079q CCC: $25.00
Published on Web 02/14/2003

and polymer purification was first distilled, then deionized to a resistance of 18 MΩ (Barnstead E-Pure system), and then filtered through a 0.2 μm filter to remove particulate matter.

Core Microgel Synthesis. Core particles were prepared via aqueous free-radical precipitation polymerization as previously reported.[2,11−13] Polymerization was performed in a three-neck, 200 mL round-bottom flask equipped with a magnetic stir bar, reflux condenser, thermometer, and nitrogen inlet. The initial total monomer concentration was held constant at 70 mM, and the comonomer ratio, (9−*X*:1:*X*) (NIPAm:AAc:BIS), was varied according to the desired cross-linker concentration. All monomers and surfactant (1 mM) were dissolved in 100 mL of H_2O and then filtered through a 0.2 μm membrane filter (Pall Gelman Metricel) to remove remaining particulate matter. The monomer/surfactant solution was heated to 70 °C under a stream of nitrogen with constant stirring at ∼850 rpm (Corning magnetic stirrer). This solution was allowed to stabilize for a period of at least 1 h prior to initiation. Free radical polymerization was then initiated with APS (0.3 mmol) dissolved in 1 mL of heated (70 °C) H_2O. The stirring solution was allowed to react for a period of 5 h under nitrogen.

Shell Synthesis. Shell addition was performed by using core particles as nuclei in the subsequent precipitation polymerization of a feed of differing monomer composition. The polymerization was carried out using the reaction conditions described above and in previous publications.[11−13] A 7.5 mL portion of the core particle solution together with 0.006 g of SDS was added to 12.0 mL of water and heated to 70 °C under nitrogen. Although core particle solutions contain SDS, added surfactant is necessary for stabilization during heating and subsequent shell polymerization. During this second stage of polymerization, the entire (shell) monomer solution is added to the core mixture under monomer-flooded conditions. Specifically, a 5.0 mL solution containing the constituent shell monomers was heated separately under nitrogen to 70 °C, which was then added to the stirring core solution. After mixing for several minutes, free radical polymerization was initiated with a 1 mL heated solution of APS (0.04 mmol) and allowed to proceed under nitrogen for 5 h. The total (shell) monomer concentration was held constant at 40 mM (in the final 25.5 mL solution) while the ratio (10−*X*:*X*) (NIPAm:BIS) was varied according to the desired cross-linker concentration. All particles used for analysis were purified via dialysis (Spectra/Por 7 dialysis membrane, MWCO 10 000, VWR) against daily changes of H_2O for 2 weeks at 5 °C.

Characterization. Particle sizes and polydispersities were determined via photon correlation spectroscopy (PCS, Protein Solutions Inc.) as previously reported.[11] All solutions used for PCS measurements were adjusted to the desired pH with HCl and/or NaOH while monitoring with a Corning 430 pH meter. Sodium chloride was then used to adjust each solution to 0.001 M total ion concentration. Particle sizes were analyzed in a three-sided quartz cuvette into which was placed 0.5 mL of a 10 μg/mL particle solution. The sample was allowed to equilibrate at the proper temperature for 5 min before data collection. Scattered light from a fiber-coupled diode laser (798 nm) was collected at 90° with a fiber-coupled avalanche photodiode detector connected to a 248-channel autocorrelator board. The data were analyzed with Protein Solutions' Dynamics Software Version 5.25.44. Each data point reported here is an average of five separate size determinations. Each size determination consists of 25 total measurements, which individually have a 5 s integration time.

Results and Discussion

Cross-linked pNIPAm microgels undergo a temperature-induced volume change at ∼31 °C, which is the intrinsic lower critical solution temperature (LCST) of the parent polymer.[2] The position, magnitude, and breadth of this continuous volume phase transition (VPT) vary with the addition of comonomers, cross-linker type, and concentration and by changes to the surrounding medium.[14,15] In the hydrophilic swollen state, water molecules surround and fill individual microgels as hydrogen bonding occurs between water and the side-chain amides. Hydrogen bonding is disrupted as the local solution temperature is increased from below to above the polymer LCST. The entropically favored expulsion of water from the polymer matrix along with hydrophobic and hydrogen-bonding interactions between neighboring polymer chains cause the particles to undergo a large-magnitude volume change. Comonomers such as acrylic acid may be incorporated into pNIPAm hydrogel systems to impart pH responsivity to the thermosensitive material.[6,16] All of the core/shell microgels reported herein contain 10 mol % acrylic acid (AAc) monomer in the core component. As shown in Figure 1, the addition of this pH responsive comonomer does not change the VPT behavior of the core microgels at pH 3.5. When the acid groups are protonated below the AAc pK_a (4.25),[17] the resultant VPT is characteristic of neutral pNIPAm microgels. Upon deprotonation of the acid groups at pH 6.5, a pH-induced volume change is apparent at all temperatures, along with a broadening of the phase transition region and a reduction in the magnitude of the deswelling event. These effects are due to both Coulombic repulsion between charged groups and added osmotic pressure (Donnan effect) from incorporated counterions.[18−20] Solution ionic strength was also considered here as having a potential impact on particle behavior. All of the experiments performed in this study were conducted in solutions containing 1 mM total ion, above which particle behavior may be perturbed by solvated ions.[21]

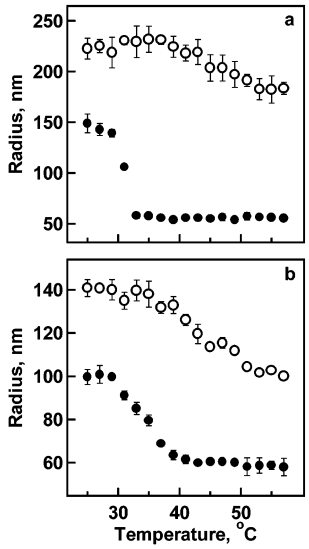

Figure 1. Temperature-induced volume phase transition behavior of pNIPAm-*co*-AAc core particles above (○, pH 6.5) and below (●, pH 3.5) the pK_a (4.25) of acrylic acid as monitored by photon correlation spectroscopy: (a) 1 mol % BIS; (b) 10 mol % BIS. Error bars represent one standard deviation about the average result of five measurements. Where error bars are not visible, the symbol size has exceeded the magnitude of the error.

As described above, the main objective of this study is to investigate the thermodynamic and morphological impact of a hydrogel shell on a hydrogel core particle. Our chosen experimental design relies upon a pH and temperature responsive core particle, upon which a temperature responsive, pH innocent material is added. In this fashion, the shell-induced modulation of the pH response and thermoresponsivity of the core particle can

be studied. We have chosen a well-investigated pH/thermoresponsive hydrogel, pNIPAm-*co*-AAc, as the core material. As we have shown in previous work, the properties of core/shell microgels containing this copolymer have properties that are not a simple sum of the individual core and shell components, suggesting that the shell strongly impacts the core behavior.[11] In this previous case, the thermodynamics of particle deswelling was investigated, whereas the mechanical properties of this core/shell system are now being presented. We have chosen to control the degree of particle solvation through the variation of cross-linker concentration, which determines the equilibrium swelling volume. More lightly cross-linked systems are typically more swollen than highly cross-linked systems, which have a denser network structure. Figure 1a,b compares the VPT behavior of lightly cross-linked (1 mol % BIS, panel a) and highly cross-linked (10 mol % BIS, panel b) pNIPAm-*co*-AAc core microgels in conditions both above and below the AAc pK_a. Since microgels with lower cross-linker content have a lower density and hence greater solvation, one would expect that the swelling properties of the more lightly cross-linked microgels (the core) would show a greater perturbation once polymer (the shell) has been added to them. Conversely, particles containing higher percentages of cross-linker, such as the 10 mol % system (Figure 1b), possess a higher internal density of polymer chains. The perturbation of the swelling behavior of the core in this case should not be as great, since the system is already highly constrained due to the cross-linked nature of the polymer network.

Cross-linker heterogeneity within individual microgels also determines particle deswelling and is a result of the preparation method. Thermal precipitation polymerization takes advantage of the physical properties of polymers possessing a lower critical solution temperature (LCST) such as pNIPAm (31 °C). Microgel particle formation occurs in aqueous solution upon temperature-induced free radical initiation with ammonium persulfate at 70 °C. At this temperature, the water-soluble monomers polymerize to form oligomers that are insoluble upon reaching a certain critical chain length. These chains undergo entropically driven coil-to-globule phase transitions and aggregate with other globules to form precursor particles, which then aggregate and grow to form colloidally stable microgels. Stabilization occurs due to both surfactant adsorption and charge incorporated on the growing particles from the initiator fragments.[2] During particle growth, the cross-linker is statistically incorporated faster than other constituent monomers, leading to the creation of a radial distribution of cross-links.[1,2,12,22,23] In light of this model, one can consider a single microgel as having an internal core/shell type structure with respect to cross-linking density; the core represents the densely cross-linked center of the particle, and the shell represents the decreasing cross-linking concentration moving outward toward the particle periphery. It has been shown that the gradient model becomes insufficient for describing the internal structure of microgels beginning at around 7 mol % cross-linker.[24] At 10 mol % BIS, the thickness of the cross-link density gradient should tend toward zero; no gradient structure is present, and any cross-linker heterogeneity that is present is no longer radial in nature.[25] The ramifications of this morphology on the impact of shell addition are related to the contribution

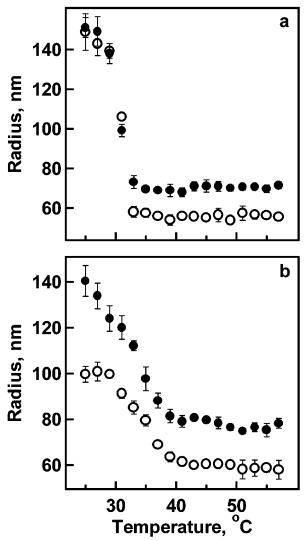

Figure 2. Volume phase transition behavior of pNIPAm-*co*-AAc core (○) and pNIPAm-*co*-AAc core/pNIPAm shell (●) microgels at pH 3.5. (a) 1 mol % BIS microgels show little size change below the polymer LCST, but a size increase at temperatures above 35 °C indicates that a shell is present. (b) 10 mol % BIS microgels show an increase in size at all temperatures following shell addition with a broader volume phase transition being observed for the core/shell microgels.

Scheme 1. Core Compression during Shell Addition

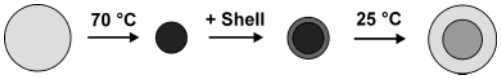

of a cross-linker gradient to the behavior of the core. Specifically, chains close to the particle periphery have more degrees of freedom and are able to extend over longer length scales in a good solvent. However, this same population of loosely cross-linked chains will be hindered from reaching their fully extended state in the presence of added polymer (e.g., the shell). The average number of chains that will be perturbed will differ according to the initial cross-linker concentration, with lower mol % cross-linked particles having a higher average number of loosely cross-linked chains near the periphery than highly cross-linked particles, which do not have a gradient morphology.[24,25] Accordingly, one would expect to see smaller shell-induced perturbations for the higher cross-linker densities than those observed for loosely cross-linked, "gradient" core particles.

Shell addition is performed via precipitation polymerization onto existing core microgels as shown in Scheme 1, with the addition of material onto the core being monitored by noting size differences between the core and core/shell particles with photon correlation spectroscopy (PCS).[11−13] Figure 2 shows the VPT behavior of the pNIPAm-*co*-AAc core microgels at pH 3.5 before and after the addition of a pNIPAm shell. The 1 mol % (panel a) and 10 mol % (panel b) BIS cross-linked samples are once again used to illustrate the effect of shell addition as a function of network density. Data from 2 and 5 mol % cross-linked microgels are included in the Supporting Information. In Figure 2a, the lightly cross-linked core/shell particles surprisingly behave quite similar to the parent core particles. The sharpness and position of the VPT remain the same for both the core and the core/shell, with the swollen particle size being identical for the two particles. A size increase is evident for the core/shell particles only at temperatures above the pNIPAm LCST. Conversely, a size increase

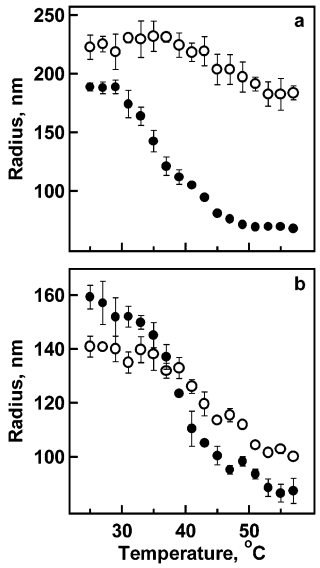

Figure 3. Volume phase transition behavior of pNIPAm-*co*-AAc core (○) and pNIPAm-*co*-AAc core/pNIPAm shell (●) microgels at pH 6.5. (a) The size of 1 mol % BIS core/shell microgels is smaller than the parent core at all temperatures, suggesting restricted swelling of the core. (b) 10 mol % BIS microgels show a slight increase in size below the polymer LCST but a size decrease above 37 °C.

is observed at all temperatures for the 10 mol % BIS core/shell microgels as shown in Figure 2b. Also noteworthy is the fact that the size difference between the core and core/shell particles at both cross-linker concentrations is ∼15 nm when the particles are fully collapsed (T > LCST). This ∼15 nm size difference is also seen for 2 and 5 mol % microgels (see Supporting Information). Together, the results shown in Figure 2 indicate that polymer was added to existing core microgels, producing a core/shell structure.

The pH 6.5 behavior of the 1 and 10 mol % cross-linked core and core/shell particles is shown in Figure 3. In contrast to the results in Figure 2, a size *decrease* is observed for the 1 mol % BIS particles following shell addition, suggesting that the pH-induced swelling of the core is now restricted by the presence of the shell. Indeed, below 31 °C, the volume of the core/shell particle is only 40% of the parent core particle volume at pH 6.5. Conversely, there is a particle size *increase* below 31 °C for the 10 mol % cross-linked particles after shell addition, as shown in Figure 3b. However, this size increase is far less than that observed for those particles at pH 3.5 (Figure 2b), again suggesting that the swelling ability of the core is modulated by the shell.

The relationship between the core and shell components can best be understood by once again considering the particle preparation method. Because the synthetic conditions are the same for shell addition, a radial cross-linking density gradient is expected to be present in the shell for BIS concentrations below 7 mol %, with the greatest network density being located at the interface between the core and shell. As illustrated in Scheme 1, collapsed core particles serve as preexisting hydrophobic nuclei and capture monomer and growing oligomers from solution in order to form the shell. Upon particle reswelling at 25 °C following shell addition, the rigid interior (more highly cross-linked portion) of the shell prohibits the core from expanding to the volume it possessed prior to shell addition. A depiction of this core/shell interface is shown in Scheme 2 and illustrates that

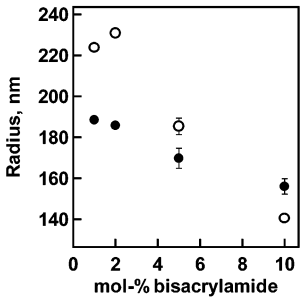

Figure 4. Average particle radii of pNIPAm-*co*-AAc core (○) and pNIPAm-*co*-AAc core/pNIPAm shell (●) microgels in their swollen state below 31 °C at pH 6.5 are shown as a function of mol % BIS cross-linker. The effects of shell-restricted swelling are greatest for microgels containing lower amounts of cross-linker.

Scheme 2. Impact of Core and Shell Crosslinker Density Gradients on Core Compression

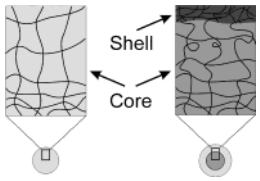

the loosely cross-linked polymer chains near the core periphery are not allowed to expand to their preshell state due to the addition of the shell. If heterogeneity were not present within both the core and shell in the form of a radial cross-linking density gradient, one would not expect to see the effects observed here, as the core and shell would have *the same average and local cross-linker concentration*.

The restricted swelling that occurs below the polymer LCST in solution conditions above the acid pK_a (pH 6.5) can be monitored over a range of cross-linker densities as presented in Figure 4. Each data point represents the average hydrodynamic radius of the core and core/shell particles below 31 °C. These data show that core particles containing lower cross-linker concentrations are perturbed to a larger degree than highly cross-linked systems. Specifically, the 1 and 2 mol % BIS core/shell particles are significantly smaller than the parent core particles, while the 5 mol % BIS microgels show a somewhat smaller size decrease. The 10 mol % BIS microgels show an inversion in the apparent trend, with the core/shell particle being slightly larger than the parent core particle. The average number of loosely cross-linked chains in the 10 mol % BIS core that are perturbed from their native swollen state by the shell is far less than in the case of the loosely cross-linked systems. The swelling ability of the core also appears to be affected even below the acid pK_a for lightly cross-linked microgels, as indicated in Figure 2a. The 1 mol % BIS cross-linked core and core/shell particles are approximately the same size in their fully swollen state. One would expect the core/shell particles to be larger than the parent core if the core were able to swell to its original volume. Thus, the effect seen here is not solely due to factors originating from the pH-responsive comonomer. We have not yet fully investigated interpenetration of polymer chains at the core/shell interface but do not believe that such behavior plays a dominant role here. This assumption is based on previous electron microscopy and fluorescence resonance energy transfer studies of core/shell microgels, which suggested only small degrees of interpenetration were present.[11,12]

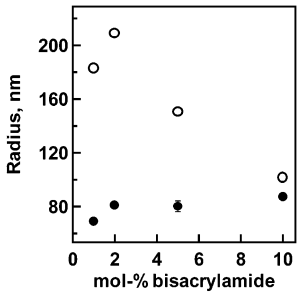

Figure 5. Average particle radii of pNIPAm-*co*-AAc core (○) and pNIPAm-*co*-AAc core/pNIPAm shell (●) microgels in their collapsed state above 52 °C at pH 6.5. Core/shell particles are smaller than the charged core for lightly cross-linked systems, an effect that decreases as the cross-linking density increases.

In addition to mediating the solvation of the core, the added pNIPAm shell also controls the overall particle deswelling behavior above the polymer LCST by forcing the charged microgel core to undergo a volume phase transition, as illustrated in Figures 3 and 5. Shown in Figure 3 is the ability of the added pNIPAm shell to compress the charged core at the LCST of neutral pNIPAm, despite the resistance of the parent core particle to deswelling when the AAc moieties are deprotonated (as shown in Figure 1). An overall volume change of 95% is observed for the 1 mol % BIS cross-linked core/shell microgels (Figure 3a) as the temperature is increased above 30 °C, which is characteristic of neutral pNIPAm systems. The VPT occurs over a broader temperature range for the lightly cross-linked core/shell particles than is typical for a neutral pNIPAm core particle, possibly due to added particle heterogeneity, the resistance of the charged core to undergo a phase transition, and limited diffusion processes mediated by the shell. The 10 mol % BIS core/shell particles are also smaller than the parent core at temperatures above 37 °C. In this case, however, the core/shell particles are only slightly smaller than the parent core, and the transition temperature is shifted to higher values, suggesting that the denser core has a greater ability to resist the deswelling of the neutral shell. However, the transition occurs over a narrower range of temperatures than is observed for the parent core, which is indicative of some thermodynamic impact of the shell addition.

It is thought that the pNIPAm shell begins to undergo a phase transition at ∼31 °C beginning at the periphery, thereby leading to a decrease in particle size. Such behavior has been demonstrated in a previous work for core/shell microgels of a similar composition.[12] As illustrated by the data discussed above, the temperature-induced phase transition of the shell is able to overcome the propensity of the charged core component to remain swollen under such conditions. Figure 5 shows this effect as a function of mol % BIS cross-linker. Each data point represents the average hydrodynamic radius of the core and core/shell particles above 52 °C. As in the case of the data in Figure 4, the deswelling effect is most pronounced for the lightly cross-linked systems. Size changes between the core and core/shell due to shell-induced compression are greater for systems containing lower cross-linker concentrations due to the lower network density within the polymer matrix. The loosely cross-linked chains near the periphery of the core are already within a closer proximity of each other due to the shell, thereby predisposing the core to undergo favorable hydrophobic interactions. As the temperature increases, chain−chain interactions begin to dominate, and the volume of the entire microgel decreases due to compression by the shell. This behavior is again attributable to the cross-linker density gradient in both the core and shell components for particles synthesized with BIS concentrations below 7 mol %. Together, these data point to the ability of the shell to strongly modulate the overall particle behavior by compressing and or restricting the core swelling.

Conclusions

Fundamental structure−function relationships have been investigated for pNIPAm-based core/shell microgels. Tailoring of the phase transition behavior for such systems is possible via the copolymerization of acrylic acid and variation of the cross-linker concentration providing added dimensionality to understanding relationships between the core and the shell. The ability of a pNIPAm-*co*-AAc core to reswell to its native volume is hindered following the addition of a pNIPAm shell. The added shell also imparts a volume phase transition and compresses the core above the pNIPAm LCST. Such structure−function relationships are important for the design of future systems to use in potential applications such as chemical sensing and controlled release.

Acknowledgment. L.A.L. gratefully acknowledges financial support from the National Science Foundation, Division of Materials Research. C.D.J. gratefully acknowledges financial support from a National Science Foundation Trainee Fellowship in Environmental Sciences and from the Polymer Education Research Center at the Georgia Institute of Technology.

Supporting Information Available: Photon correlation spectroscopy data as a function of pH and temperature for 2 and 5 mol % *N*,*N*′-methylenebis(acrylamide) (BIS) cross-linked core/shell particles. This material is available free of charge via the Internet at http://pubs.acs.org.

References and Notes

(1) Saunders, B. R.; Vincent, B. *Adv. Colloid Interface Sci.* **1999**, *80*, 1−25.
(2) Pelton, R. *Adv. Colloid Interface Sci.* **2000**, *85*, 1−33.
(3) Holtz, J. H.; Holtz, J. S. W.; Munro, C. H.; Asher, S. A. *Anal. Chem.* **1998**, *70*, 780−791.
(4) Hoffman, A. S. *Adv. Drug Deliv. Rev.* **2002**, *54*, 3−12.
(5) Bergbreiter, D. E.; Case, B. L.; Liu, Y. S.; Caraway, J. W. *Macromolecules* **1998**, *31*, 6053−6062.
(6) Morris, G. E.; Vincent, B.; Snowden, M. J. *J. Colloid Interface Sci.* **1997**, *190*, 198−205.
(7) Duracher, D.; Elaissari, A.; Mallet, F.; Pichot, C. *Langmuir* **2000**, *16*, 9002−9008.
(8) Jeong, Y. I.; Cheon, J. B.; Kim, S. H.; Nah, J. W.; Lee, Y. M.; Sung, Y. K.; Akaike, T.; Cho, C. S. *J. Controlled Release* **1998**, *51*, 169−178.
(9) Zheng, W. X.; Maye, M. M.; Leibowitz, F. L.; Zhong, C. J. *Anal. Chem.* **2000**, *72*, 2190−2199.
(10) Kalinina, O.; Kumacheva, E. *Macromolecules* **1999**, *32*, 4122−4129.
(11) Jones, C. D.; Lyon, L. A. *Macromolecules* **2000**, *33*, 8301−8306.
(12) Gan, D.; Lyon, L. A. *J. Am. Chem. Soc.* **2001**, *123*, 8203−8209.
(13) Gan, D.; Lyon, L. A. *J. Am. Chem. Soc.* **2001**, *123*, 7511−7517.
(14) Duracher, D.; Elaissari, A.; Pichot, C. *Macromol. Symp.* **2000**, *150*, 305−311.
(15) Crowther, H. M.; Vincent, B. *Colloid Polym. Sci.* **1998**, *276*, 46−51.
(16) Yoo, M. K.; Sung, Y. K.; Lee, Y. M.; Cho, C. S. *Polymer* **2000**, *41*, 5713−5719.

(17) Lide, D. R. *Handbook of Chemistry and Physics*, 74th ed.; CRC Press: Boca Raton, FL, 1913−1995.
(18) Flory, P. J. *Principles of Polymer Chemistry*; Cornell University Press: Ithaca, NY, 1953.
(19) Fernandez-Nieves, A.; Fernandez-Barbero, A.; Vincent, B.; de las Nieves, F. J. *Macromolecules* **2000**, *33*, 2114−2118.
(20) Ito, S.; Ogawa, K.; Suzuki, H.; Wang, B. L.; Yoshida, R.; Kokufuta, E. *Langmuir* **1999**, *15*, 4289−4294.
(21) Daly, E.; Saunders, B. R. *Phys. Chem. Chem. Phys.* **2000**, *2*, 3187−3193.
(22) Wu, X.; Pelton, R. H.; Hamielec, A. E.; Woods, D. R.; McPhee, W. *Colloid Polym. Sci.* **1994**, *272*, 467−477.
(23) Wu, C.; Zhou, S. Q. *Macromolecules* **1997**, *30*, 574−576.
(24) Varga, I.; Gilanyi, T.; Meszaros, R.; Filipcsei, G.; Zrinyi, M. *J. Phys. Chem. B* **2001**, *105*, 9071−9076.
(25) Guillermo, A.; Addad, J. P. C.; Bazile, J. P.; Duracher, D.; Elaissari, A.; Pichot, C. *J. Polym. Sci., Part B: Polym. Phys.* **2000**, *38*, 889−898.

MA021079Q